Mol Cell Biochem (2008) 309:177–189
DOI 10.1007/s11010-007-9658-4

Transient and sustained oxidative stress differentially activate the JNK1/2 pathway and apoptotic phenotype in H9c2 cells

Anastasia Pechtelidou · Isidoros Beis · Catherine Gaitanaki

Received: 3 September 2007 / Accepted: 14 November 2007 / Published online: 4 December 2007

Abstract The aim of this study was to investigate the activation of JNK1/2 signalling pathway and the respective cellular phenotype of H9c2 cardiac myoblasts during two distinct types of oxidative insult. We examined the dose- and time-dependent activation of JNK1/2 pathway by exogenous H_2O_2, both under transient and sustained stimulation. At 2 h of either sustained or transient treatment, maximal phosphorylation of c-Jun was observed, coincidently with the activation of nuclear JNK1/2; under sustained stress, these phosphorylation levels remained elevated above basal for up to 6 h, whereas under transient stress they declined to basal ones within 4 h of withdrawal. Furthermore, the JNK1/2 selective inhibitor SP600125 abolished the c-jun phosphorylation induced by oxidative stress. Our results using cell viability assays and light microscopy revealed that sustained H_2O_2 stimulation significantly and time-dependently decreased H9c2 viability, in contrast to transient stimulation; SP600125 (10 μM) abolished cell death induced by sustained as well as cell survival induced by transient oxidative stress. Hoechst staining showed an increase in DNA condensation during sustained, but not during transient stimulation. Moreover, from the antioxidants tested, catalase and superoxide dismutase prevented oxidative stress-induced cell death. Flow cytometry studies reconfirmed that sustained oxidative stress induced apoptosis, whereas transient resulted in the recovery of cardiac myoblasts within 24 h. We conclude that in H9c2 myoblasts, sustained activation of JNK1/2 signalling pathway during oxidative stimulation is followed by an apoptotic phenotype, while transient JNK1/2 activation correlates well with cell survival, suggesting a dual role of this signalling pathway in cell fate determination.

Keywords H9c2 · JNKs - c-Jun · Apoptosis · Oxidative stress · Signal transduction · Cardiac myoblast

Abbreviations

7-AAD	7-Amino actinomycin D
AP-1	Activating protein-1
ASK1	Apoptosis signal-regulating kinase-1
BSA	Bovine serum albumin
CAT	Catalase
DMSO	Dimethylsulfoxide
DTT	Dithiothreitol
ECL	Enhanced chemiluminescence
ERK	Extracellular signal-regulated kinase
FBS	Fetal bovine serum
HOX-1	Heme oxygenase-1
JNK	c-Jun N-terminal kinase
MAPK	Mitogen-activated protein kinase
MKK	MAPK kinase
MKKK	MAPK kinase kinase
MTT	3-(4.5-dimethyl-thiazol-2yl)-2.5-diphenyl tetrazolium bromide
NFκB	Nuclear factor κB
PAGE	Polyacrylamide gel electrophoresis
P-PDA	p-Phenylen-diamine
PMSF	Phenyl methyl sulfonyl fluoride
PBS	Phosphate buffered saline
PI	Propidium iodide
ROS	Reactive oxygen species
SOD	Superoxide dismutase

A. Pechtelidou · I. Beis · C. Gaitanaki (✉)
Department of Animal and Human Physiology, School of Biology, Faculty of Sciences, University of Athens, Panepistimioupolis, Athens 157 84, Greece
e-mail: cgaitan@biol.uoa.gr

TBS	Tris-buffered saline
TNF-α	Tumor necrosis factor alpha
Trx	Thioredoxin

Introduction

Oxidative stress has been defined as a disturbance in the pro-oxidant/antioxidant balance, resulting in potential cell damage. Aerobic organisms are continuously exposed to reactive oxygen species (ROS), including superoxide anion (O_2^-), hydroxyl ion (OH^-) and hydrogen peroxide (H_2O_2) [1]. During oxidative stress, an increase in intracellular ROS leads to irreversible damage of various cellular components, such as lipids, proteins and DNA [2]. Increasing evidence shows that cellular ROS act as secondary messengers in intracellular signalling cascades; however, ROS can also induce cellular senescence and apoptosis [3]. Apoptosis is a complex form of cell death, characterized by cell shrinkage, chromatin condensation, internucleosomal DNA fragmentation and formation of apoptotic bodies [4].

A number of intracellular signal transduction pathways are regulated by variations in cellular redox status, such as the mitogen-activated protein kinase (MAPK) family members and nuclear factor κB (NF-κB) [5]. ROS are critical messengers participating in the regulation of MAPK-dependent apoptotic pathway by different signalling systems [6]. The three well-established subfamilies that constitute the MAPK family (the extracellular signal-regulated kinases-ERKs, the c-Jun N-terminal kinases-JNKs and the p38-MAPK) [7] have been directly implicated in regulating aspects of cardiac myocyte apoptosis [8]. JNKs appear to be pro-apoptotic and experimental data suggests that JNK1/2 signalling is involved in apoptosis secondary to oxidative stress [9], tumor necrosis factor alpha (TNF-α) [10] and in animal models of acute myocardial infarction [11]. Nevertheless, other studies have suggested a protective role of JNKs [12, 13], and the duration of their induction may be crucial in mediating the signalling decision [14–16].

Direct treatment of cells with oxidants such as H_2O_2 was thought to exclusively cause necrosis, but more recent studies have shown that ROS can trigger apoptosis under certain circumstances [2, 3]. Many previous studies on the induction of apoptosis by H_2O_2 actually employed a long-term exposure paradigm, while in vivo, transient exposure of cells to H_2O_2 is a frequently encountered situation, as in the case of acute myocardial ischemia and reperfusion [17].

In the present study, H9c2 cardiac myoblasts—a clonal cell line derived from embryonic rat heart ventricle [18]—were used as an experimental model, since they have been proven to be ideal for signal transduction studies [19, 20]. The aim of our study was to investigate the exact pattern of JNK1/2 pathway activation during two types of oxidative insult in H9c2 cells: sustained exposure to H_2O_2 and transient exposure followed by a subsequent time of stimulus withdrawal. In parallel, we aimed to examine the respective cellular phenotype under these two experimental conditions as well as whether JNK1/2 signalling pathway is related with these distinguishable differences between the two types of stress. As positive controls for cell death evaluation, H9c2 myoblasts treated with either 10 mM H_2O_2 or 400 μM $CoCl_2$ were used. Cobalt chloride is a well-known hypoxia mimetic agent [21] that has been demonstrated to act as a pro-oxidant, inducing an increase in the levels of ROS [22–24] in diverse cell types [25, 26]. Finally, we also examined the protective effects of three known antioxidant substances, L-ascorbic acid, catalase and superoxide dismutase (SOD), on the apoptotic cell death induced by sustained oxidative stress.

Materials and methods

Materials

All chemicals were of analytical grade and purchased from Sigma-Aldrich Co, Merck and Applichem. Hoechst 33258 was purchased from Molecular Probes (Invitrogen). Protein concentration was determined using the Bradford protein assay reagent from BioRad Laboratories; prestained protein markers were from New England Biolabs Inc.; nitrocellulose from Schleicher & Schuell. Rabbit polyclonal antibodies against the dually phosphorylated (Thr183/Tyr185) JNK1/2, the phosphorylated (Ser63) c-Jun and total (phosphorylation state independent) c-Jun were from Cell Signaling Technology; the antibody against the actin N-terminus was from Sigma-Aldrich Co; the secondary antibody (goat anti-rabbit HRP-conjugated) was from DAKO; the enhanced chemiluminescence (ECL) western blot reagent kit was from Amersham Biosciences; the X-ray SuperRX (18 × 24 cm) was from Fuji Film. Flow cytometry materials were obtained from Becton Dickinson.

Cell culture

The H9c2 embryonic rat heart-derived cell line [18] was obtained from the American Type Culture Collection (CRL-1446) and cultured in growth medium comprising DMEM (High glucose-PAA Laboratories GmbH) supplemented with 10% (v/v) of heat-inactivated fetal bovine serum (FBS) (PAA Laboratories, GmbH), 100 U/ml

penicillin and 0.1 mg/ml streptomycin (Gibco). Cells were grown in an atmosphere of 95% O_2/5% CO_2 in a humidified incubator and passaged at a 1:4 ratio.

For all experiments, except for viability assays and morphological examination, cells were plated at the appropriate density 2 days before experimentation. For the preparation of whole cell extracts and subcellular fractionation, plating density was 3×10^5 cells/petri dish (35 mm) and 1.2×10^6 cells/petri dish (100 mm), respectively. For fluorescent nuclear staining, 5×10^3 cells were plated onto slides in a 24-well plate. For viability assays and microscopic examination, 10^4 cells were plated in 96-well plates 24 h prior to experimentation.

Oxidative stress treatments

Cells were treated with H_2O_2 by addition of the oxidant to the culture medium using two distinct protocols: a transient 5 min exposure to H_2O_2 followed by increasing times of withdrawal (*transient conditions*) and a prolonged stimulation for desired time periods (*sustained conditions)*. For the transient protocol, cells were washed with Ca^{++}- Mg^{++}-free phosphate-buffered saline (PBS) prior to the addition of fresh culture medium (withdrawal). Treatment with antioxidants at appropriate concentrations (500 μM L-ascorbic acid, 75 U/ml catalase and 30 U/ml SOD) or with the JNK1/2 selective inhibitor SP600125 (2.5 and 10 μM) was performed 30 min prior to the addition of H_2O_2.

Preparation of whole cell extracts and subcellular fractionation

For whole cell extraction, cells were harvested in Buffer G [50 mM Hepes, 2 mM EDTA, 20 mM NaF, 0.2 mM Na_3VO_4, 20 mM β-glycerophosphate, 0.2 mM leupeptin, 5 mM dithiothreitol (DDT), 0.3 mM phenylmethylsulfonyl fluoride (PMSF), 10 μM trans-epoxysuccinyl-L-leucylamido-(4-guanidino)butane (E64), 0.5% (v/v) Triton X-100] and incubated on ice for 30 min. After centrifugation (4°C, 10 min, 10,000 g), samples were prepared for Western blot analysis.

For preparation of nuclear fractions, cells were harvested into Buffer A [10 mM Hepes, 10 mM KCl, 0.1 mM EGTA, 0.1 mM EDTA, 1.5 mM $MgCl_2$, 10 mM NaF, 1 mM Na_3VO_4, 20 mM β-glycerophosphate, 2 μg/ml leupeptin, 1 mM DDT, 0.5 mM PMSF, 4 μg/ml aprotinin] and incubated for 15 min on ice. Samples were centrifuged (4°C, 5 min, 1,400 g), pellets were washed in Buffer A containing 0.6% (v/v) Nonidet P40 and nuclear proteins were extracted in Buffer B [20 mM Hepes, 0.4M NaCl, 1 mM EGTA, 0.1 mM EDTA, 1.5 mM $MgCl_2$, 10 mM NaF, 1 mM Na_3VO_4, 20 mM β-glycerophosphate, 2 μg/ml leupeptin, 0.2 mM DDT, 0.5 mM PMSF, 4 μg/ml aprotinin] for 1 h, under stirring at 4°C, and obtained in the supernatant by a final centrifugation (4°C, 10 min, 11,000 g).

For Western blot analysis, whole cellular or nuclear extracts were boiled with 0.33 vol. of SDS sample buffer [0.3M Tris–HCl, pH 6.8, 10% (w/v) SDS, 13% (v/v) glycerol, 20% (v/v) β-mercaptoethanol, 0.2% (w/v) bromophenol blue].

Western blot analysis

Proteins from whole cellular (20 μg) or nuclear extracts (40 μg) were separated by SDS-PAGE on 10% polyacrylamide gels. Proteins were transferred electrophoretically onto nitrocellulose membranes (0.45 μm). Nonspecific sites were blocked by incubating membranes (30 min, room temperature) in 5% (w/v) non-fat milk powder in Tris-buffered saline containing 0.05% (v/v) Tween 20 (TBS-T). Blots were incubated with primary antibodies against phospho-JNK1/2, β-actin, c-Jun, or phospho-c-Jun, diluted in 5% (w/v) BSA in TBS-T (1:1,000 dilution, 16 h, 4°C). Membranes were washed in TBS-T and incubated with HRP-linked antibodies diluted in 5% (w/v) non-fat milk in TBS-T (1:5,000 dilution, 1 h, room temperature). Blots were washed in TBS-T and bands were visualized using an ECL kit according to the manufacturer's instructions. Bands were semi-quantitatively analysed using scanning densitometry.

Cell viability assays

Cell viability was measured using the MTT bioreduction assay [27] in the absence or presence of various antioxidants. Cells were treated with H_2O_2 for the desired time periods (*sustained or transient exposure*). Four hours prior to the end of treatment, 3-(4.5-dimethyl-thiazol-2yl)-2.5-diphenyl tetrazolium bromide (MTT) substrate diluted in sterile PBS was added in each chamber at a final concentration of 0.4 mg/ml, and cells were kept in the incubator (37°C). At end of the reaction, chamber growth medium was discarded, blue crystals were dissolved in 100 μl of 0.1 M HCl in isopropanol, and the absorbance at 545 nm was read using an ELISA plate-reader.

In another series of experiments, cell viability was assessed by staining with propidium iodide (PI) which penetrates damaged membranes and intercalates to nuclear DNA. H9c2 cells were treated with 400 μM H_2O_2 for either 24 h (*sustained exposure*) or for 5 min followed by

24 h of withdrawal (*transient exposure*), both in the absence or presence of the JNK1/2 selective inhibitor SP600125 (10 μM). About 30 min prior the end of treatments, propidium iodide was added at a dilution of 1:2,000. Coverslips were washed 3 times in PBS, mounted and observed under a Zeiss Axioplan fluorescence microscope (20× magnification) equipped with an AxioCam MRc5.

Microscopic examination of cell death

In order to qualitatively examine cell death, cells were exposed to H_2O_2 as above and observed under an optical microscope (10× magnification). Photographs were taken with a camera appropriately adjusted to the microscope (NOVA IN834 Trinocular inverted microscope). A suitable film for coloured slides (Kodak ektachrome 400×) was used. As positive controls cells treated for 24 h with 10 mM H_2O_2 or 400 μM $CoCl_2$ were used.

Fluorescent staining of nuclei

Cells were cultured onto cover slips in 24-well plate chambers for 48 h prior to treatment with H_2O_2. After the desired treatment, growth medium was removed and in each chamber 300 μl of medium containing 10 μg/ml Hoechst 33258 were added. Cover slips were incubated for 15 min, washed with PBS and covered with 300 μl of mounting medium (P-PDA: p-phenylen-diamine). Cells were observed (40× magnification) under a fluorescence microscope (Zeiss-Axioplan). Photographs were taken from all conditions with a camera appropriately adjusted to the microscope, using a suitable film for coloured slides (Kodak ektachrome 400×).

Flow cytometry

Annexin and 7-AAD (7-amino actinomycin D) staining was performed in conjunction with flow cytometry to confirm the above used methods of apoptosis detection on a larger, unselected population of cells using the Annexin V-PE Apoptosis Detection Kit. This assay takes advantage of the binding by annexin to phosphatidyl-serine residues exposed on the cell surface soon after induction of apoptosis before nuclear breakdown occurs (when 7-AAD staining is present). H9c2 cells were plated on 60 mm dishes for 2 days, at which time they were treated with H_2O_2 as above. About 6 or 24 h later, cells were collected by trypsinisation and suspended in PBS. All subsequent steps were performed with the cells and reagents on ice. Cells were pelleted and washed once more in binding buffer (10 mM Hepes/NaOH, pH 7.4, 140 mM NaCl and 2.5 mM $CaCl_2$) before the addition of 2.5 μl annexin V-PE and 2.5 μl 7AAD and were incubated for 15 min in the dark. Cells were assayed by flow cytometry using FACSCalibur™ (BD) and CellQuest analysis software, with results positive or negative for both 7AAD and annexin. Viable cells do not stain with either reagent, early apoptotic cells stain with annexin only, and either late apoptotic or necrotic cells stain with both annexin and 7AAD. Because we were mainly interested in the number of cells that were clearly apoptotic, cells positive for annexin alone were compared on the basis of treatment condition.

Statistical evaluation

Western blots were scanned using Adobe Photoshop 6.0 and bands were semi-quantified by Gel Analyzer 1.0. JNK1/2 and c-Jun phosphorylation levels were normalized against total protein levels and in untreated cells were set as 1, while JNK1/2 and c-Jun activation in treated cells was expressed as "fold" activation or increase over control values. Statistical analysis of all results was conducted for at least three independent experiments using GraphPad Prism 4.0 and the Student's *t*-test with 95% level of certainty (P-values <0.05 are considered to be significant). Results of all experiments are presented as mean ± standard error for at least three independent experiments.

Results

As the first step in the present study, we made an effort to examine the dose- and time-dependent phosphorylation pattern of p54 and p46 JNKs during a sustained or a transient stimulation by exogenous H_2O_2 in H9c2 cardiac myoblasts.

In order to assess the dose-dependent response of JNK1/2, cardiac myoblasts were incubated with increasing concentrations of H_2O_2 either continuously for 2 h (100–1,000 μM), or transiently (40–1,000 μM) for 5 min followed by 15 min of withdrawal. Under these different experimental conditions, activation of p54 and p46 showed different dose-dependent patterns. In particular, sustained exposure to 200 μM of the oxidant resulted in a moderate phosphorylation of both kinase isoforms, with a maximal phosphorylation attained at 400 μM of H_2O_2 [7.64 ± 0.46-fold ($P < 0.001$) and 5.47 ± 0.44-fold relative to control values for p54 and p46, respectively] (Fig. 1a top panel, Fig. 1b). During the transient stimulation with 100 μM H_2O_2, we observed a strong activation of p54 and p46 JNKs, with maximal phosphorylation detected at 400 μM of the oxidant [7.95 ± 0.34-fold and 4.37 ± 0.52-fold

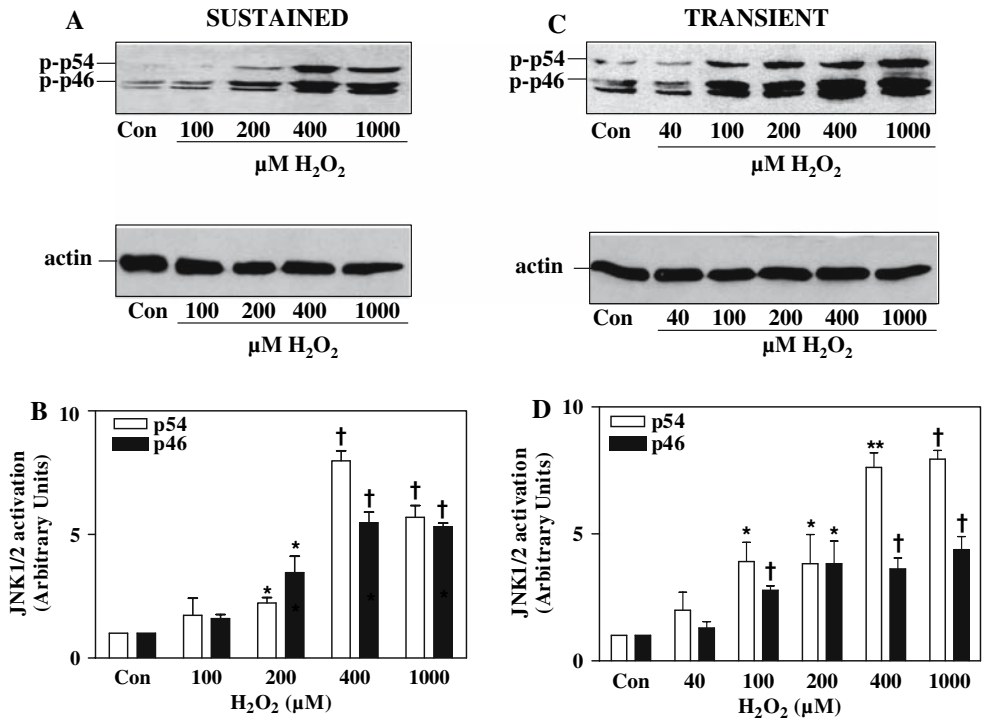

Fig. 1 Dose–response of JNK1/2 phosphorylation during sustained and transient oxidative stress. H9c2 cells were exposed either under sustained (for 2 h) (**a**) or transient conditions (5 min treatment followed by 15 min of withdrawal) (**c**) to the indicated H_2O_2 concentrations. Protein extracts (20 μg) were separated by SDS-PAGE and blotted using an antibody specific for the dually phosphorylated isoforms of JNK1/2. **a** and **c**, *top panels*: Dose–response of phospho JNK1/2. **a** and **c**, *bottom panels*: Western blots for equal loading were performed using an antibody against actin. Western blots shown are representative of three independent experiments. (**b**) and (**d**): Densitometric analysis of phospho JNK1/2 bands by laser scanning. Results are means ± S.E.M. for three independent experiments performed with similar findings. $^*P < 0.05$, $^{**}P < 0.01$, †$P < 0.001$, vs. control (Con) values

above basal ($P < 0.001$), for p54 and p46, respectively] (Fig. 1c top panel, Fig. 1d). For all experiments described in this study, a concentration of 400 μM H_2O_2 was chosen based on the above results. Equivalent protein loading was confirmed by probing identical samples with antibodies recognizing the actin protein levels (Fig. 1a and c, bottom panels).

In another series of experiments, the time-dependent profile of JNK1/2 activation by 400 μM H_2O_2 was examined. H9c2 cells were continuously stimulated with the oxidant for increasing time periods varying from 1 up to 4 h, or transiently for 5 min followed by increasing time periods of withdrawal, varying from 15 min up to 4 h. Under sustained oxidative conditions (Fig. 2a top panel, Fig. 2b), both p54 and p46 JNKs highly attained maximal activation at 2 h of treatment (7.80 ± 0.28 and 5.61 ± 0.52-fold relative to control values, $P < 0.001$, for p54 and p46, respectively). The kinases preserved high activation levels even after 4 h of treatment, thus for the experiments of sustained stimulation we decided to expose the cells to H_2O_2 for 2 h. On the contrary, JNK1/2 activation with respect to time was different during transient oxidative stress (Fig. 2c top panel, Fig. 2d). In particular, both p54 and p46 JNKs were maximally activated within 15 min of withdrawal following a 5 min treatment with 400 μM H_2O_2 (8.72 ± 2.09-fold, $P < 0.05$ and 2.77 ± 0.09-fold, $P < 0.001$, for p54 and p46, respectively) and remained significantly above basal for 60 min, reaching control values within 4 h of withdrawal. These distinct time-dependent activation patterns could suggest a differential role of JNK1/2 pathway under the aforementioned conditions. Equivalent protein loading was confirmed by probing identical samples with antibodies recognizing the actin protein levels (Fig. 2a and c, bottom panels).

We further examined the time-dependent phosphorylation pattern of JNK1/2 substrate, c-Jun. For this purpose, cells were exposed to H_2O_2 for increasing time periods or for 5 min with a subsequent recovery for respective time periods. Western blot analysis was conducted in the nuclear fraction using an antibody specific for the phosphorylated c-Jun (Ser63) (Fig. 3a, top panel). From the two main bands detected by this antibody, the one of reduced mobility possibly represents an even more highly phosphorylated c-Jun form [28]. As shown in Fig. 3a (top panel), 400 μM H_2O_2 induced a maximal phosphorylation

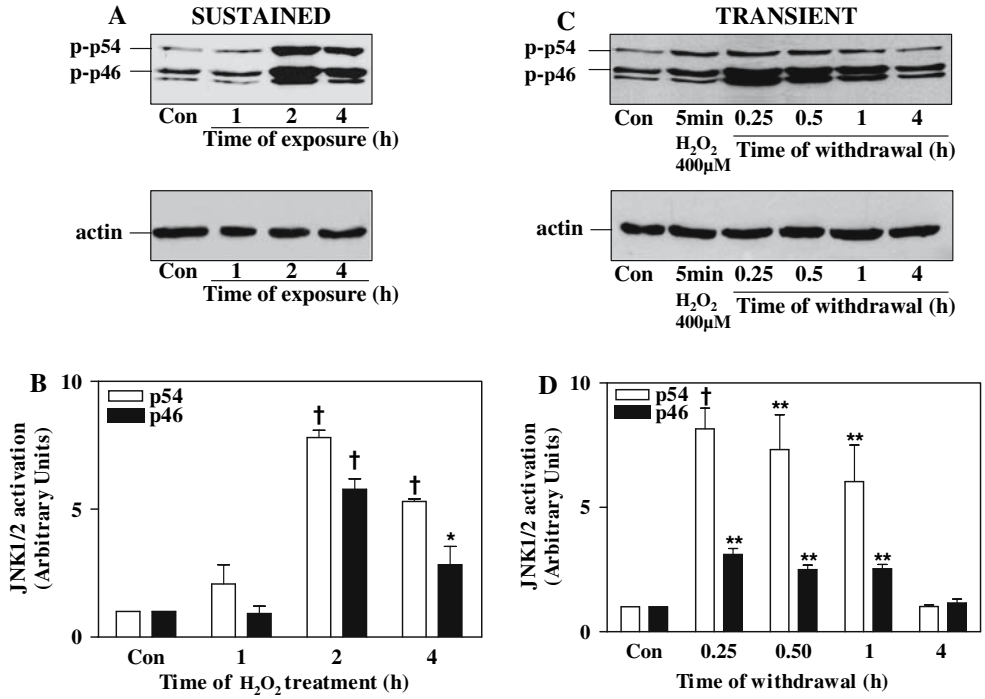

Fig. 2 Time-dependent response of JNK1/2 phosphorylation during sustained and transient oxidative stress. (**a**) Sustained exposure to 400 μM H_2O_2 (for 1, 2 or 4 h) and (**c**) transient exposure to H_2O_2 (5 min) followed by the indicated time periods of withdrawal. Protein extracts (20 μg) were assessed by immunoblot analysis using a phospho-specific anti-JNK1/2 antibody (**a** and **c**, *top panels*) or an antibody specific for actin (**a** and **c**, *bottom panels*). Western blots shown are representative of three independent experiments. (**b**) and (**d**): Densitometric analysis of phospho JNK1/2 bands by laser scanning. Results are means ± S.E.M. for three independent experiments performed with similar findings. $*P < 0.05$, $**P < 0.01$, $\dagger P < 0.001$ vs. control (Con) values

of c-Jun at 2 h of sustained stimulation (3.88 ± 0.24-fold relative to control values, $P < 0.001$), while c-Jun phosphorylation levels remained elevated even after 6 h of exposure. By contrast, during transient stress (Fig. 3a top panel, Fig. 3b), c-Jun was maximally phosphorylated at 2 h of withdrawal (3.85 ± 0.12-fold above basal, $P < 0.001$), with a progressive decline thereafter, reaching control values within 4 h of recovery. Equivalent protein loading was confirmed by probing identical samples with antibodies recognizing total c-Jun levels (both the phosphorylated and the unphosphorylated form) in the nuclear extracts under these conditions (Fig. 3a, bottom panel).

In parallel, we investigated the profile of activated JNK1/2 in the nuclear extracts during sustained and transient H_2O_2 stimulation, to deduce whether they comply with the levels of phosphorylated c-Jun. As shown in Fig. 3 (c, d), both JNK isoforms preserved high phosphorylation levels in the nucleus under sustained H_2O_2 stimulation (up to 6 h), displaying maximal phosphorylation at 2 h of treatment (6.73 ± 0.81-fold, $P < 0.01$ and 4.38 ± 0.35-fold, $P < 0.05$ relative to control values, for p54 and p46, respectively). On the contrary, transient stimulation (Fig. 3c, e) induced a significant increase of both, p54 (2.83 ± 0.3-fold above basal, $P < 0.01$) and p46 (5.04 ± 0.36-fold above basal, $P < 0.001$) phosphorylation levels at 2 h, which reached control values at 4 h of withdrawal.

We further examined the effect of the JNK1/2 selective inhibitor SP600125 on the phosphorylation of c-jun. For this purpose, cells were treated with 400 μM H_2O_2 for 2 h in the absence or presence of the inhibitor at a concentration of either 2.5 or 10 μM, respectively. The results of these experiments revealed that 2.5 μM of SP600125 had a moderate effect whereas 10 μM of this inhibitor abolished the c-jun phosphorylation induced by 400 μM H_2O_2 (Fig. 4a top panel, Fig. 4b. Equivalent protein loading was confirmed by probing identical samples with antibodies recognizing total c-Jun levels (both the phosphorylated and the unphosphorylated form) in the nuclear extracts under these conditions (Fig. 4a, bottom panel).

It was of particular interest to examine H9c2 cell viability under sustained and transient experimental conditions. In order to assess cell viability, we conducted the MTT assay during sustained oxidative stress for increasing time periods varying from 6 up to 24 h or after 5 min of transient stress and respective times of withdrawal (Fig. 5A). As positive controls, cells treated for 24 h with either 10 mM H_2O_2 or 400 μM $CoCl_2$ were included. The results of this study revealed that sustained stimulation

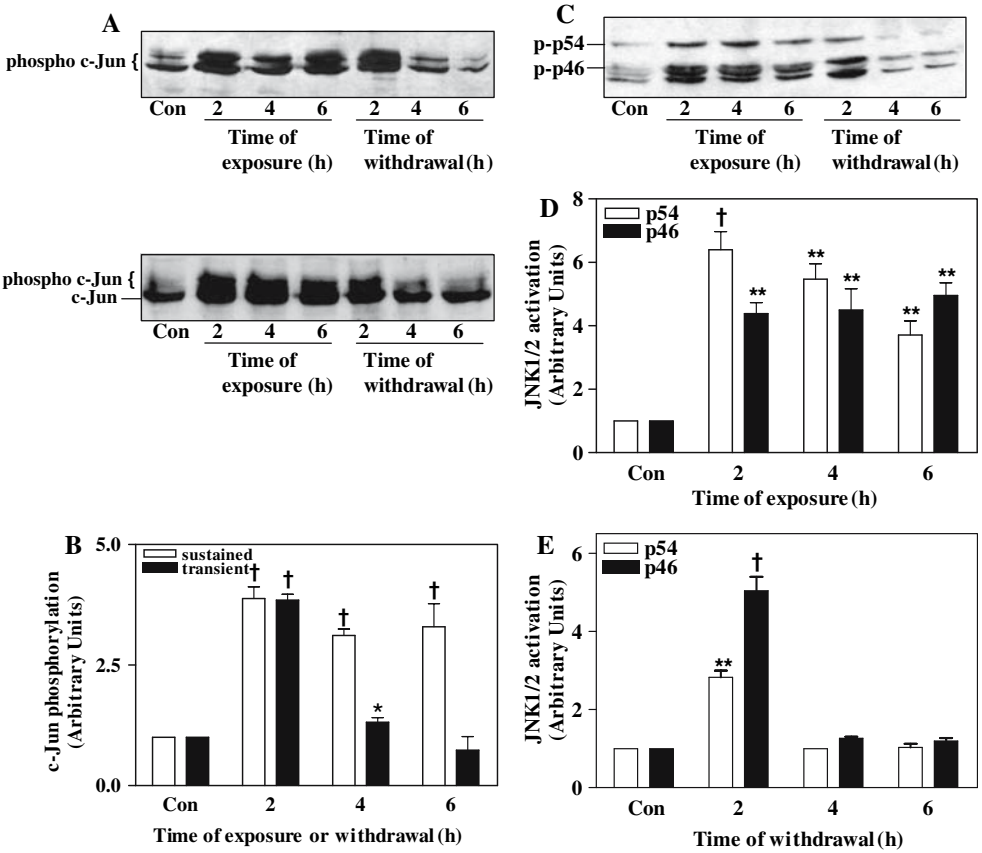

Fig. 3 Time-dependent phosphorylation of c-Jun and JNK1/2 in nuclear extracts during sustained and transient oxidative stress. Sustained exposure to 400 μM H_2O_2 was performed for 2, 4 or 6 h and transient exposure for 5 min followed by the indicated times of withdrawal. Nuclear proteins (40 μg) were assessed using an antibody specific to either phospho c-Jun (**a**, *top panel*), total c-Jun (**a**, *bottom panel*) or phospho JNK1/2 (**c**). Western blots shown are representative of four independent experiments. Densitometric analysis of phospho c-Jun (**b**), and phospho JNK1/2 bands under either sustained (**d**) or transient treatment conditions (**e**) by laser scanning. Results shown are means ± S.E.M. for four independent experiments performed with similar findings. $*P < 0.05$, $**P < 0.01$, $\dagger P < 0.001$ vs. control (Con) values

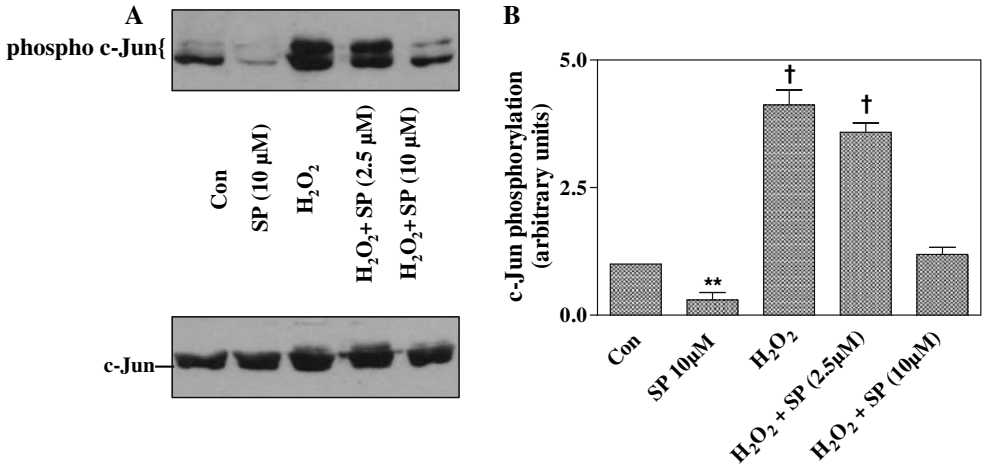

Fig. 4 Effect of the JNK1/2 selective inhibitor SP600125 on the c-Jun phosphorylation induced by sustained oxidative stress. Sustained exposure to 400 μM H_2O_2 was performed for 2 h either in the absence or presence of increasing SP600125 concentrations (2.5 and 10 μM). Nuclear proteins (40 μg) were assessed using an antibody specific to either phospho c-Jun (**a**, *top panel*) or total c-Jun (**a**, *bottom panel*). Western blots shown are representative of four independent experiments. (**b**) Densitometric analysis of phospho c-Jun by laser scanning. Results shown are means ± S.E.M. for four independent experiments performed with similar findings. $**P < 0.01$, $\dagger P < 0.001$ vs. control (Con) values

caused a significant and progressive induction of cell death. In particular, 6 h of treatment resulted in a high drop of viability (52.93 ± 10.01%, $P < 0.01$) with the lowest viability observed at 24 h of stress (32.00 ± 3.26%, $P < 0.001$) as compared to the viability of control cells (100%). On the contrary, transient oxidative stress caused a moderate death at 6 h of withdrawal, inducing a drop in viability down to 83.90 ± 2.27% ($P < 0.01$). The magnitude of cell death became lower as the time of withdrawal increased, and cells seemed to completely recover after

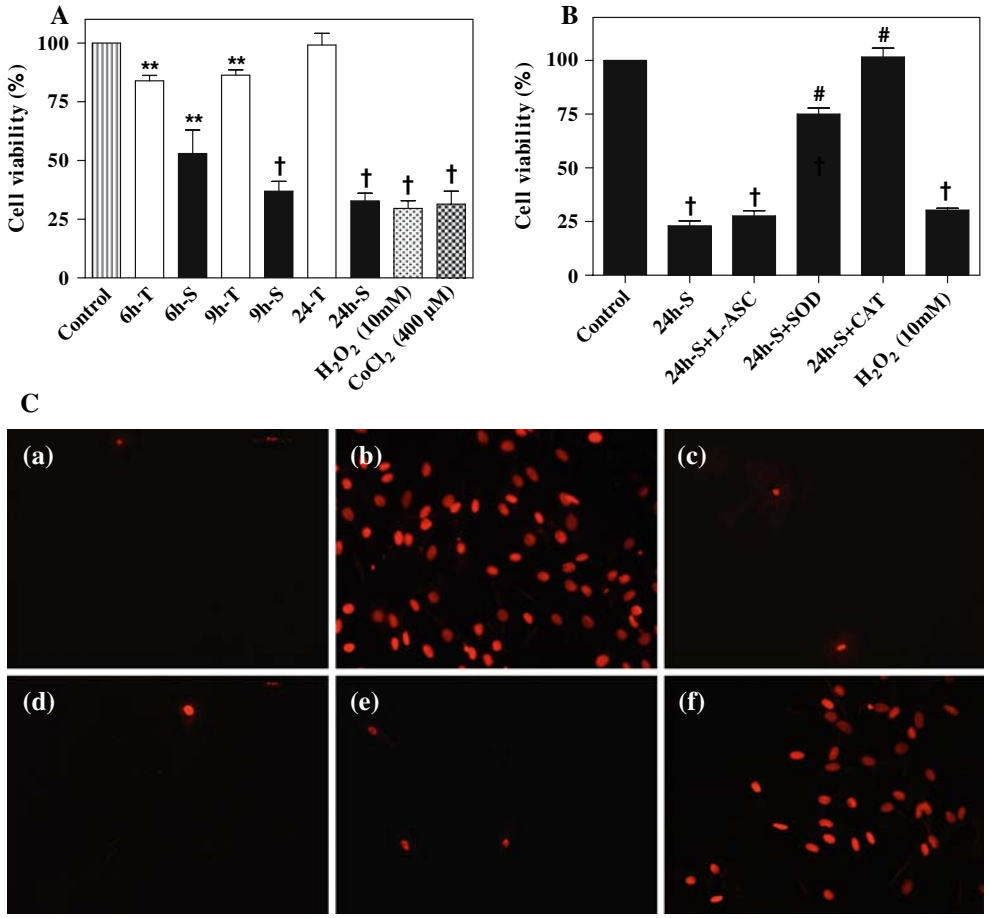

Fig. 5 Effect of sustained and transient oxidative stress on H9c2 cell viability in the absence or presence of various antioxidants and SP600125. (**A**) Percentage (%) of viable cells during sustained exposure (row S) or transient exposure (row T) to 400 μM H_2O_2 for the indicated time periods using the MTT method. As positive controls, cells treated with 10 mM H_2O_2 or 400 μM $CoCl_2$ were used. Results shown are means ± S.E.M. for three independent experiments performed with similar findings: ** $P < 0.01$, † $P < 0.001$. (**B**) Percentage (%) of viable cells during sustained exposure (row S) to 400 μM H_2O_2 for 24 h in the absence or presence of 500 μM L-ascorbic acid (L-ASC), 75 U/ml catalase (CAT) or 30 U/ml SOD using the MTT method. Results shown are means ± S.E.M. for three independent experiments performed with similar findings. †$P < 0.001$ vs. control (Con) values; # $P < 0.001$ vs. values observed after treatment of cells with 400 μM H_2O_2 for 24 h. (**C**) Cells were grown on slides and exposed to 400 μM H_2O_2 either continuously for 24 h, or for 5 min followed by 24 h of withdrawal, both in the absence or presence of the JNK1/2 selective inhibitor SP600125. Viability of cells was assessed by fluorescence microscopy using the propidium iodide staining of dead cells. (**a**) Control, (**b**) sustained exposure, (**c**) transient exposure, (**d**) cells treated with 10 μM SP600125 for 24 h, (**e**) sustained exposure in the presence of 10 μM SP600123, (**f**) transient exposure in the presence of 10 μM SP600123. Representative photographs were taken with a camera adjusted to a fluorescence microscope. Pictures are representative of four independent experiments. Magnification (20×)

24 h of withdrawal, displaying similar viability with control cells (99.10 ± 4.96%). This differential profile of metabolically viable cells under the two distinct protocols is consistent with the time-dependent activation pattern of the JNK1/2 pathway demonstrated in Figs. 2 and 3.

By using the same assay, we next tested the efficacy of three known antioxidant substances, L-ascorbic acid, catalase and SOD, towards cells exposed continuously to H_2O_2 for 24 h (Fig. 5B). None of the antioxidants showed any cytotoxic influence at the concentrations used (data not shown). Pretreatment of H9c2 cells with L-ascorbic acid exhibited no protective effect during sustained stimulation, resulting in low percentages of viability (27.66 ± 2.33%, $P < 0.001$ compared to the control values). Pretreatment with 30 U/ml SOD resulted in a significant increase of cell viability (80.10 ± 5.50, $P < 0.001$ compared to the values observed under sustained oxidative exposure) whereas catalase caused a complete cell viability recovery (113.66 ± 8.97%, $P < 0.001$ compared to the values observed under sustained oxidative exposure).

In order to elucidate the possible role of JNK1/2 signalling pathway for cell survival or death, we assessed cell viability under either sustained (24 h) or transient (5 min followed by 24 h of withdrawal) oxidative stress in the absence or presence of the selective JNK1/2 inhibitor SP600125, using the propidium idodide staining assay. The

results of this study showed that cells exposed to 400 μM H_2O_2 for 24 h were heavily stained by propidium iodide, indicating an extensive cell death (Fig. 5Cb). Furthermore, the JNK1/2 selective inhibitor SP600125 (10 μM) abolished this propidium iodide staining under sustained exposure (Fig. 5Ce). On the contrary, transient exposure to oxidative stress resulted in cell survival (Fig. 5Cc) and SP600125 (10 μM) induced a significant increase in propidium iodide staining, thus cell death (Fig. 5Cf). As controls untreated cells or cells treated with the respective inhibitor alone were included (Fig. 5Ca and 5Cd, respectively). The above results reveal the possible involvement of JNK1/2 signalling pathway in cell survival or death during oxidative stress.

In parallel to the viability assay, we conducted morphological examination of H9c2 cells under the optical microscope after 24 h of sustained or transient oxidative stress (Fig. 6A). Consistent with the results of the MTT assay, cells displayed an apoptotic phenotype at 24 h of continuous stress (Fig. 6Ab). In particular, they were detached from the solid surface and had a round, irregular morphology with an abnormal plasma membrane and an obvious shrinkage, in contrast to control cells (Fig. 6Aa). However, cells during transient exposure (Fig. 6Ac) were visibly healthy, rod-shaped and evenly covering the solid surface, resembling control cells. As positive controls for cell death, we again used 10 mM H_2O_2 or 400 μM $CoCl_2$ (Fig. 6Ad and e, respectively).

For the purpose of further investigating whether the observed cell death was due to apoptosis or necrosis, we chose to conduct fluorescent nuclear staining using Hoechst 33258. In Fig. 6B representative pictures of cells treated with 400 μM H_2O_2 either continuously for 24 h or transiently for 5 min followed by a 24 h recovery in the absence or presence of the antioxidants mentioned above are shown. Compared to the control cells (Fig. 6Ba), cells subjected to sustained oxidative stress showed an increase in nuclear fluorescence, implying apoptosis, with visible chromatin condensation and changes in the nuclear membrane morphology (Fig. 6Bb). On the contrary, cells subjected to transient stress showed no effect in the nuclear morphology as assessed by Hoechst staining (Fig. 5Bc). Furthermore, cells pretreated with either catalase or SOD showed a mild, blue fluorescence, suggesting that they are

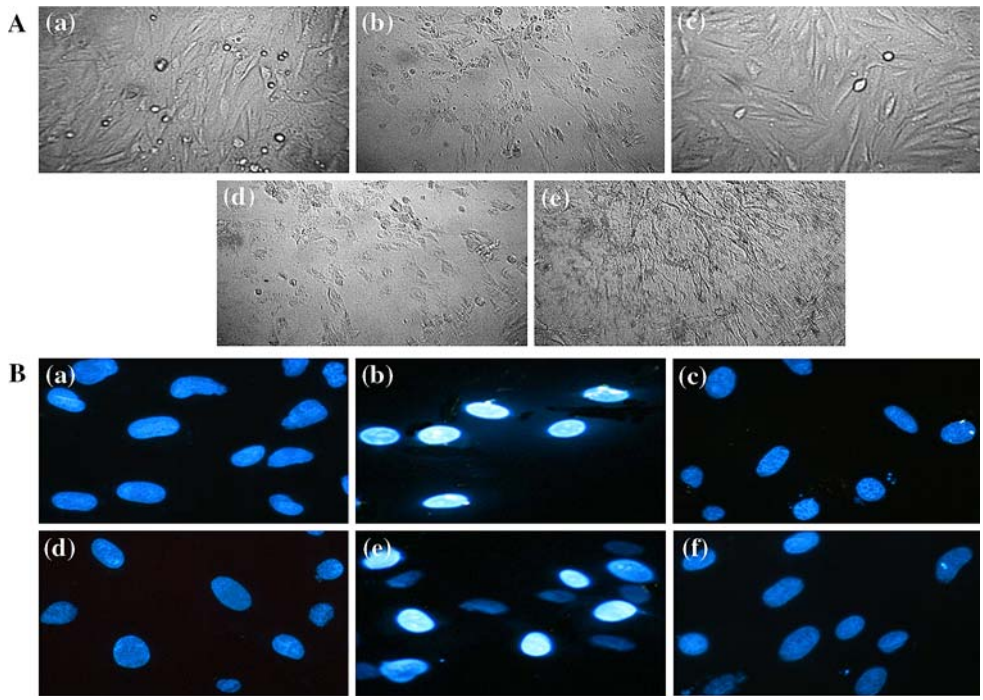

Fig. 6 Effect of sustained or transient oxidative stress on H9c2 cellular morphology (**A**), nuclear morphology using Hoechst staining (**B**). (**A**) Cells were grown in a 96-well plate and exposed to 400 μM H_2O_2 either continuously for 24 h (sustained exposure) or for 5 min with 24 h of withdrawal in fresh medium (transient exposure). Representative photographs were taken with a camera adjusted to an optical microscope: (**a**) Control, (**b**) sustained exposure, (**c**) transient exposure, (**d**) 10 mM H_2O_2 (24 h) and (**e**) 400 μM $CoCl_2$ (24 h). Magnification (10×). (**B**) Cells were grown on slides in a 96-well plate and exposed to 400 μM H_2O_2 continuously for 24 h (sustained exposure) either in the absence or presence of various antioxidants, or for 5 min followed by 24 h of withdrawal in fresh medium (transient exposure). Representative photographs were taken with a camera adjusted to a fluorescence microscope. (**a**) Control, (**b**) sustained exposure, (**c**) transient exposure, (**d**) sustained exposure in the presence of 75 U/ml catalase, (**e**) sustained exposure in the presence of 500 μM L-ascorbic acid and (**f**) sustained exposure in the presence of 30 U/ml SOD. Magnification (40×)

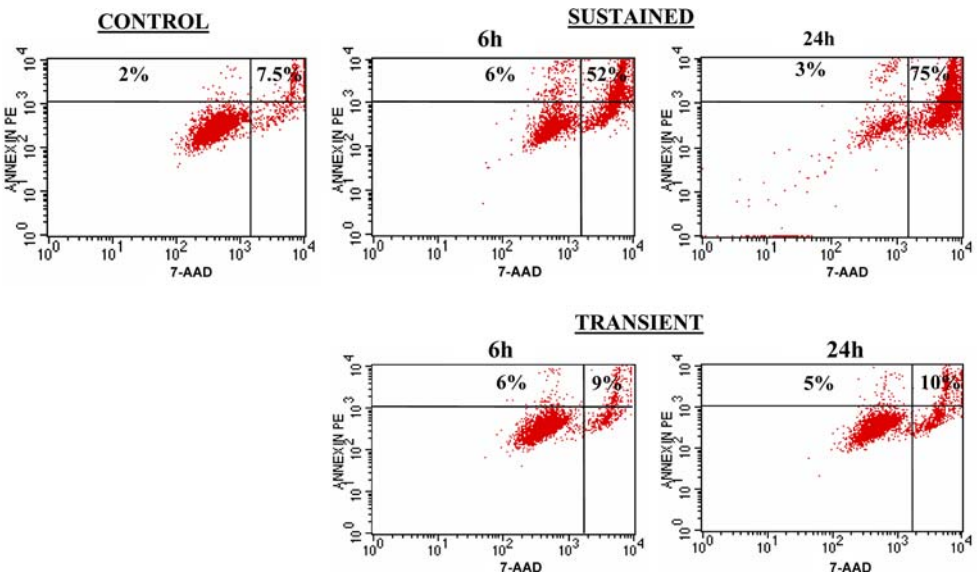

Fig. 7 Flow cytometry analysis of apoptosis in H9c2 cells treated with H_2O_2. H9c2 cells were plated on 60 mm dishes for 2 days, at which time they were treated either continuously with 400 μM H_2O_2 for 6 and 24 h (sustained exposure) or for 5 min followed by 6 and 24 h of withdrawal (transient exposure) and assayed by flow cytometry as described in the Materials and Methods section. As controls, cells incubated for 24 h in the absence of any oxidant were used. A representative scattergram of three independent experiments with similar findings is shown

healthy viable cells (Fig. 6Bd and 6Bf, for catalase and SOD, respectively). By contrast, L-ascorbic acid showed no anti-apoptotic effect (Fig. 6Be). These results, taken together with the viability assay ones and the morphological examination analysed earlier, imply the induction of an apoptotic process during sustained H_2O_2 stimulation, which is not evident during transient stress. Since JNK1/2 follow a differential activation pattern under the two distinct experimental conditions used and SP600125 abolishes the detrimental cell death after sustained exposure or the beneficial effect of transient exposure, these results suggest that prolonged JNK1/2 pathway activation is related with a H_2O_2-induced cell death, whereas transient activation of this signalling pathway is related with a H_2O_2-induced cell survival.

Annexin staining, indicative of exposure of phosphoserine residues, is an additional hallmark of an apoptotic cell death. Flow cytometry confirmed that cells treated with 400 μM H_2O_2 under both sustained or transient conditions stained positive for annexin, consistent with apoptosis (Fig. 7). The proportion of early apoptotic cells was less than 10% even after 24 h of either sustained or transient oxidative stress and higher than the control (untreated) cells (Fig. 7, upper left region in each panel). Moreover, long-term exposure led to a significant number of cells entering the late apoptotic stage (Fig. 7, upper right region in each panel), starting from 6 h of oxidative stress (∼52%) and reaching a percentage of 75% at 24 h of treatment. On the other hand, the proportion of healthy cells was maintained high during transient oxidative stress even after 24 h of withdrawal (∼78%) whereas this proportion dropped to approximately 16 and 12% during the sustained oxidative stress for 6 and 24 h, respectively (Fig. 7, lower left region in each panel). The sum of these results is consistent with the previously presented data on apoptotic phenotype examination and indicates that apoptosis and necrosis occur depending on the duration of the stimulus. Namely, transient stress causes a small percentage of cells to enter the early apoptotic stage displaying annexin-V exposure (Fig. 7), but no changes in nuclear and cellular morphology (Fig. 6A, B), while sustained stress leads to a significant proportion of cells to proceed through apoptosis (Figs. 6B, 7).

Discussion

Extracellular addition of H_2O_2 has been previously shown to activate MAPK pathways and the apoptotic process [3, 29]. All three well-established MAPK cascades have been directly implicated in regulating aspects of cardiac myocyte apoptosis [8], and JNK signalling has been suggested to have both pro-apoptotic [10, 11, 30] and anti-apoptotic effects [12, 13]. In this study, we directly investigated the activation pattern of JNK1/2 during short or prolonged oxidative treatment of H9c2 cardiac myoblasts with exogenous H_2O_2. Our results show that both JNK isoforms are strongly activated during treatment with increasing concentrations of H_2O_2, under both sustained and transient conditions (Fig. 1). Activation of JNK1/2 can be attributed to the fact that ROS induce the apoptosis signal-regulating kinase-1 (ASK1)- an MKKK of the JNK module- through dissociation of its endogenous inhibitor thioredoxin (Trx) [6, 29].

Small changes in the duration of JNK1/2 activation can produce major changes in survival [9]. In our experimental model, the activation of JNK1/2 is prolonged under continuous treatment with 400 μM H_2O_2 (Fig. 2), a result

consistent with previous reports [20, 31, 32]. By contrast, short-term treatment causes an early activation of JNK1/2 during withdrawal, suggesting a transient activation of this pathway that might serve a physiological role. Transient JNK activity during oxidative treatment has been reported previously [17], but to our knowledge our study is the first to characterise the activation pattern of JNK1/2 pathway in H9c2 cells under these two distinct types of oxidative stimulation, revealing an interesting differential profile.

A growing body of evidence suggests that H_2O_2 can modulate transcription factors, such as activating protein-1 (AP-1) and NF-κB [1]. The transcription factor c-Jun is a basic component of AP-1 and the main substrate of JNK1/2 [7]. Our results demonstrate a respective time-dependent pattern of c-Jun phosphorylation (Fig. 3), in support to the differential profile of activated JNK1/2 in the whole cell extract (Fig. 2) and the nuclear fraction (Fig. 3c, d) under the same conditions. Furthermore, the JNK1/2 selective inhibitor SP600125 abolishes the c-Jun phosphorylation induced by oxidative stress (Fig. 4). The prolonged activation of c-Jun during sustained oxidative challenge could have a physiological meaning in the cellular context, since AP-1 is associated with a large number of apoptotic scenarios [33]. However, the precise role of AP-1 in response to JNK activation is likely to be modified by the activity of other transcription factors that interact with AP-1 on the promoters of target genes [15]. By contrast, during transient oxidative stress both phosphorylated p54 and p46 JNKs were detected in the nucleus only at 2 h of withdrawal (Fig. 3c, e), a pattern that largely resembles the transient c-Jun phosphorylation (Fig. 3a, b) under such conditions.

Nevertheless, it is not known whether the aforementioned nuclear phosphorylated isoforms represent a fraction of activated JNK1/2 that translocates to the nucleus or whether they are derived from phosphorylation in the nucleus by specific MAPK kinases (MKKs). In resting cells, JNK1/2 are localized in both the cytoplasm and the nucleus [34], thus the nuclear isoforms we detected could be indeed phosphorylated within the latter.

Subsequent studies to investigate the phenotype of H9c2 cells under the two distinct experimental protocols were in accordance with the pattern of JNK1/2 activation mentioned previously. Sustained H_2O_2 treatment resulted in a significant percentage of cell death and an apoptotic phenotype, as assessed by viability assays (Fig. 5A, C), microscopic examination (Fig. 6A) and Hoechst 33258 staining (Fig. 6B). On the contrary, during transient stimulation there was only a small and transient impact on cell survival (Fig. 5A, C), and no obvious phenotypical changes as compared to control cells (Fig. 6A, B). In addition, the abolishment of either cell death during sustained or cell survival during transient stimulation by the JNK1/2 selective inhibitor SP600125 (Fig. 5C), provides evidence for a direct link between this signalling pathway and cell fate determination. Moreover, flow cytometry experiments (Fig. 7) showed a small percentage of early apoptosis during transient stimulation in contrast to substantial number of late apoptotic cells during sustained oxidative episode, in compliance with the above morphological data. Our results comply with other studies that have reported a significant decrease in cell viability during oxidative insults [35, 36]. They are also consistent with previous reports on increased Hoechst staining [13, 36, 37] or pathological phenotype [17, 37, 38] of cardiac myocytes under different types of sustained oxidative stress. From the antioxidants tested, catalase and SOD were able to prevent the observed cell death and apoptotic phenotype under sustained conditions (Figs. 5B, 6B).

Overall, the results of the present study demonstrate that JNK isoforms are strongly activated in H9c2 cardiac myoblasts during both sustained and transient oxidative stimulation. Nevertheless, their time-dependent profile is different under these two distinct conditions of stress, in consistence with the pattern of their phosphorylated substrate, c-Jun. During the short-term oxidative episode, transient activation of JNK1/2 correlates well with a survival phenotype. Nonetheless, during prolonged H_2O_2 treatment, sustained JNK1/2 activation is followed by a pathological cellular phenotype with well-established apoptotic hallmarks.

Our results suggest that stress-dependent JNK1/2 activation might be implicated in diverse cellular responses, by signalling in favour of either survival or apoptosis [15]. The mechanisms of this dual role of JNK have been discussed in a number of reviews [6, 8, 15]. In addition, a recent study in our laboratory reported a JNK and p38-MAPK-dependent up-regulation of heme oxygenase-1 (HOX-1) in H9c2 cells treated with 200 μM H_2O_2, thus implicating JNK in the mechanisms preserving cellular homeostasis [39].

A critical factor determining cell fate is thought to be the duration of JNK activation, with transient JNK activation mediating a survival response and prolonged JNK activation contributing to apoptotic responses [14, 16]. Moreover, the dynamic balance between ERK and JNK pathways is important in determining whether a cell survives or undergoes apoptosis [14, 40]. Therefore, it is likely that the differences in sensitivity of various cell types to the cytotoxic effects of H_2O_2 reflect the relative activation of ERK and JNK [9]. A third explanation for the different roles of JNK in apoptosis signalling is that the cellular outcome may depend on the cross talk with other signal transduction pathways (e.g. NF-κB and Akt). For example, target genes of the anti-apoptotic NF-κB pathway may contain JNK-responsive elements in their promoters

(e.g. AP-1 sites), as has been shown for inhibitory of apoptosis protein (cIAP) [41].

In conclusion, the present study demonstrates that transient and sustained oxidative stress can cause differential JNK pathway activation, resulting in cell survival or apoptosis, respectively, in accordance with previous studies on UV-C [14] and TNF-α treatment [10, 42]. Clearly, a greater understanding of the regulatory role of JNK1/2 pathway in apoptosis may reveal additional strategies for treating heart failure, cardiomyopathy and acute ischemic heart damage in humans, and Dr A. Gritzapis for his assistance in FACS analyis.

Acknowledgements This study was funded by O.P.E.I.V.T. II. We thank Vasilis Varvarigos for his kind assistance in fluorescence microscopy examination, and Dr A. Gritzapis for his assistance in FACS analysis.

References

1. Haddad JJ (2002) Antioxidant and prooxidant mechanisms in the regulation of redox(y)-sensitive transcription factors. Cell Signal 14:879–897
2. Marczin N, El-Habashi N, Hoare GS, Bundy RE, Yacoub M (2003) Antioxidants in myocardial ischaemia- reperfusion injury: therapeutic potential and basic mechanisms. Arch Biochem Biophys 420:222–236
3. Valko M, Leibfritz D, Moncol J, Cronin MTD, Mazur M, Telser J (2007) Free radicals and antioxidants in normal physiological functions and human disease. Int J Biochem Cell Biol 39:44–84
4. Kumar D, Jugdutt BI (2003) Apoptosis and oxidants in the heart. J Lab Clin Med 142:288–297
5. Allen RG, Tresini M (2000) Oxidative stress and gene regulation. Free Radic Biol Med 28:463–499
6. Sumbayev VV, Yasinska IM (2005) Regulation of MAP kinase-dependent apoptotic pathway: implication of reactive oxygen and nitrogen species. Arch Biochem Biophys 436:406–412
7. Kyriakis JM, Avruch J (2001) Mammalian MAPKs signal transduction pathways activated by stress and inflammation. Physiol Rev 81:807–869
8. Baines CP, Molkentin JD (2005) Stress signalling pathways that modulate cardiac myocyte apoptosis. J Mol Cell Cardiol 38:47–62
9. Wang X, Martindale JL, Holbrook NJ (1998) The cellular response to oxidative stress: influences of mitogen-activated protein kinase signalling pathways on cell survival. Biochem J 333:291–300
10. Guo YL, Baysal K, Kang B, Yang LJ, Williamson JR (1998) Correlation between sustained c-Jun N-terminal protein kinase activation and apoptosis induced by tumor necrosis factor-a in rat mesangial cells. J Biol Chem 273:4027–4034
11. Li GW, Zaheer A, Coppey L, Oskarsson HJ (1998) Activation of JNK in the remote myocardium after large myocardial infarction in rats. Biochem Biophys Res Commun 246:816–820
12. Dougherty CJ, Kubasiak LA, Prentice H, Andreka P, Bishopric NH, Webster KA (2002) Activation of c-Jun N-terminal kinase promotes survival of cardiac myocytes after oxidative stress. Biochem J 362:561–571
13. Engelbrecht AM, Niesler C, Page C, Lochner A (1996) p38 and JNK have distinct regulatory functions on the development of apoptosis during simulated ishaemia and reperfusion in neonatal cardiomyocytes. Basic Res Cardiol 99:338–350
14. Chen YR, Wang X, Templeton D, Davis RJ, Tan TH (1996) The Role of c-jun N-terminal kinase (JNK) in apoptosis induced by ultraviolet C and γ radiation. J Biol Chem 271:31929–31936
15. Davis RJ (2000) Signal transduction by the JNK group of MAP kinases. Cell 103:239–252
16. Lamb JA, Ventura JJ, Hess P, Flavell RA, Davis RJ (2003) JunD mediates survival signaling by the JNK signal transduction pathway. Mol Cell 11:1479–1489
17. Han H, Long H, Wang H, Wang J, Zhang Y, Wang Z (2004) Progressive apoptotic cell death triggered by transient oxidative insult in H9c2 rat ventricular cells: a novel pattern of apoptosis and the mechanisms. Am J Physiol Heart Circ Physiol 286: H2169–H2182
18. Kimes BW, Brandt BL (1976) Properties of a clonal muscle cell line from rat heart. Exp Cell Res 98:367–381
19. Su C, Chong K, Edelstein K, Lille S, Khardori R, Lai C (1999) Constitutive hsp70 attenuates hydrogen peroxide-induced membrane lipid peroxidation. Biochem Biophys Res Commun 265:279–284
20. Turner NA, Xia F, Azhar G, Zhang X, Liu L, Wei JY (1998) Oxidative stress induces DNA fragmentation and caspase activation via the JNK pathway in H9c2 cardiac muscle cells. J Mol Cell Cardiol 30:1789–1801
21. Goldberg MA, Dunning SP Bunn HF (1988) Regulation of erythropoietin gene: evidence that the oxygen sensor is a heme protein. Science 242:1412–1415
22. Zou W, Yan M, Xu W, Huo H, Sun L, Zheng Z, Liu X (2001) Cobalt chloride induces PC12 cells apoptosis through reactive oxygen species and accompanied by AP-1 activation. J Neurosci Res 64:646–653
23. Xi L, Taher M, Yin C, Salloum F, Kukreja RC (2004) Cobalt chloride induces delayed cardiac preconditioning in mice through selective activation of HIF-1a and AP-1 and iNOS signaling. Am J Physiol Heart Circ Physiol 287:H2369–H2375
24. Kotake-Nara E, Saida K (2006) Endothelin-2/vasoactive intestinal contractor: regulation of expression via reactive oxygen species induced by CoCl2 and biological activities including neurite outgrowth in PC12 cells. Scientific World J 6:176–186
25. Tomaro ML, Frydman J, Frydman RB (1991) Heme oxygenase induction by CoCl2, Co-protoporphyrin IX, phenylhydrazine, and diamide: evidence for oxidative stress involvement. Arch Biochem Biophys 286:610–617
26. Chandel NS, McClintock DS, Feliciano CE, Wood TM, Melendez JA, Rodriguez AM, Schumacker PT (2000) Reactive oxygen species generated at mitochondrial complex III stabilize hypoxia-inducible factor 1a during hypoxia. J Biol Chem 275:25130–25138
27. Denizot F, Lang R (1986) Rapid colorimetric assay for cell growth and survival. Modifications to the tetrazolium dye procedure giving improved sensitivity and reliability. J Immunol Method 89:271–277
28. Clerk A, Kemp TJ, Harrison JG, Mullen AJ, Barton PJR, Sugden PH (2002) Up-regulation of c-Jun mRNA in cardiac myocytes requires the extracellular signal-regulated kinase cascade, but c-Jun N-terminal kinases are required for efficient up-regulation of c-Jun protein. Biochem J 368:101–110
29. Takeda K, Matsuzawa A, Nishitoh H, Ichijo H (2003) Roles of MAPKKK ASK1 in stress-induced cell death. Cell Struct Funct 28:23–29
30. Aikawa R, Komuro I, Yamazaki T, Zou Y, Kudoh S, Tanaka M, Shiojima I, Hiroi Y, Yazaki T (1997) Oxidative stress activates extracellular signal-regulated kinases through Src and Ras in cultured cardiac myocytes of neonatal rats. J Clin Invest 100:1813–1821
31. Hong F, Kwon SJ, Jhun BS, Kim SS, Ha J, Kim SJ, Sohn NW, Kang C, Kang I (2001) IGF-1 protects H9c2 cardiac myoblasts

from oxidative stress-induced apoptosis via PI3K and ERK pathway. Life Sci 68:1095–1105
32. Mizukami Y, Okamura T, Miura T, Kimura M, Mogami K, Todoroki-Ikeda N, Kobayashi S, Matsuzaki M (2001) Phosphorylation of proteins and apoptosis induced by JNK1 activation in rat cardiomyocytes by H2O2 stimulation. Biochim Biophys Acta 1540:213–220
33. Ameyar M, Wisniewska M, Weitzman JB (2003) A role for AP-1 in apoptosis: the case for and against. Biochimie 85:747–752
34. Whitmarsh AJ, Davis RJ (1996) Transcription factor AP-1 regulation by mitogen-activated protein kinase signal transduction pathways. J Mol Med 74:589–607
35. Chen HW, Chien CT, Yu SL, Lee YT, Chen WJ (2002) Cyclosporine A regulates oxidative stress-induced apoptosis in cardiomyocytes: mechanisms via ROS generation, iNOS and Hsp70. Brit J Pharmacol 137:771–781
36. Park C, So HS, Shin CH, Baek SH, Moon BS, Shin SH, Lee HS, Lee DW, Park R (2003) Quercetin protects the hydrogen peroxide-induced apoptosis via inhibition of mitochondrial dysfunction in H9c2 cardiomyoblast cells. Biochem Pharmacol 66:1287–1295
37. Yue TL, Wang C, Romanic A, Kikly K, Keller P, DeWolf WE, Hart TK, Thomas HC, Storer B, Gu JL, Wang X, Feuerstein GZ (1998) Staurosporine-induced apoptosis in cardiomyocytes: a potential role for caspase-3. J Mol Cell Cardiol 30:495–507
38. Chen QM, Tu VC, Wu Y, Bahl JJ (2000) Hydrogen peroxide dose dependent induction of cell death or hypertrophy in cardiomyocytes. Arch Biochem Biophys 373:242–248
39. Aggeli IK, Gaitanaki C, Beis I (2006) Involvement of JNKs and p38-MAPK/MSK1 pathways in H_2O_2-induced upregulation of heme oxygenase-1 mRNA in H9c2 cells. Cell Signal 18:1801–1812
40. Xia Z, Dickens M, Raingeaud J, Davis RJ, Greenberg ME (1995) Opposing effects of ERK and JNK–p38 MAP kinases on apoptosis. Science 270:1326–1331
41. Hong SY, Yoon WH, Park JH, Kang SG, Ahn JH, Lee TH (2000) Involvement of two NF-kappa B binding elements in tumor necrosis factor alpha-, CD40-, and Epstein-Barr virus latent membrane protein 1-mediated induction of the cellular inhibitor of apoptosis protein 2 gene. J Biol Chem 275:8022–18028
42. Roulston A, Reinhard C, Amiri P, Williams LT (1998) Early activation of c-Jun N-terminal kinase and p38 kinase regulate cell survival in response to tumor necrosis factor-α. J Biol Chem 273:10232–10239